Metal-insulator transition in the half-filling two-orbital Hubbard model on the triangular lattice

Feng Lu,[1,2] Wei-Hua Wang,[1,3] and Liang-Jian Zou[1]
[1]*Key Laboratory of Materials Physics, Institute of Solid State Physics, Chinese Academy of Sciences, P.O. Box 1129, Hefei 230031, People's Republic of China*
[2]*Graduate School of the Chinese Academy of Sciences, Beijing 100049, People's Republic of China*
[3]*Department of Electronics, College of Information Technical Science, Nankai University, Tianjin 300071, People's Republic of China*
(Received 26 September 2007; revised manuscript received 18 February 2008; published 12 March 2008)

We have investigated the half-filled two-orbital Hubbard model on a triangular lattice by means of the dynamical mean-field theory. The local squared moments of charge, spin, and orbital and the optical conductivity clearly show that the metal-insulator transition (MIT) occurs at U_c, U_c=18.2, 16.8, 6.12, and 5.85 for Hund's coupling J=0, 0.01U, $U/4$, and $U/3$, respectively. The distinct continuities of the double occupation of electrons, the local squared moments, and the local susceptibility of charge, spin, and orbital suggest that for $J>0$, the MIT is first-order; however, at $J=0$, the MIT is second order. We attribute the first-order nature of the MIT to the symmetry lowering of the systems with finite Hund's coupling.

DOI: 10.1103/PhysRevB.77.125117 PACS number(s): 71.30.+h, 64.60.−i

I. INTRODUCTION

Metal-insulator transitions (MITs) and related properties in correlated electron systems have been the central topics in condensed matter physics for several decades.[1] The MIT can be easily realized by the variation of the external fields, doping concentration, pressure, and temperature in many typical transition-metal oxides. The simplest and effective model to describe the low-energy physics of these strongly correlated transition-metal oxides is the single-orbital Hubbard model, including the competition between the kinetic energy and the local Coulomb interaction. Such a competition may result in many complicated and novel phenomena, such as the high temperature superconductivity in low-dimensional cuprates. Theoretically, great progress has been achieved in understanding the essence of the MIT in the single-orbital Hubbard model, mainly due to the development of the dynamical mean-field theory[2] (DMFT) in the past decade. The DMFT allows us to accurately treat the Hubbard subbands in the frequency axis and to obtain the quasiparticle peaks with the three-peak structure, which makes this approach an advance over the density functional theory and the Hartree-Fock approximation.[3] With the help of DMFT, we have gotten a deep insight to many properties of the single-orbital Hubbard model, e.g., the MIT, the optical conductivity and absorption, transport, and so on.[3] Among these properties related to the MIT, the order of the MIT in the Hubbard model is essential. Bulla *et al.*[4,5] demonstrated that in the single-orbital Hubbard model on the Bethe lattice, the MIT is first order for $0<T<T_c$, while it is second order for $T>T_c$. In the two-dimensional Hubbard model, Onoda and Imada[6] also found that the MIT is first order in finite $T<T_{MIT}$ by means of the correlator projection approach with the DMFT. These suggest that in low T, the MIT in the single-orbital Hubbard model is first order.

Since the realistic transition-metal oxides, such as manganites, vanadates, titanates, and nickelates, usually have multiple degenerate orbitals,[7] the multiorbital Hubbard model is more appropriate to describe the low-energy processes than the single-orbital Hubbard model. At the same time, the multiorbital Hubbard model may exhibit more complicated and richer phenomena than the single-orbital Hubbard model. Besides the conventional localization-delocalization transition of electrons, there may exist many different orbital ordered phases. For example, in a two-orbital system, one orbital may be completely empty and another is filled, forming the ferro-orbital and/or antiferro-orbital ordered phase, or one orbital is filled and insulating, another is partially occupied and metallic, forming the so-called orbital selective Mott phase.[8–12] In these situations, the orbital degree of freedom plays an important role in the phase diagram and the ground-state properties.

More recently, a number of researches have been concentrated on the nature of MIT and other properties of the two-orbital Hubbard models.[13–16] However, even on the Bethe or the hypercubic lattices, the nature of the MIT in the two-orbital Hubbard models has been controversial, although intensive theoretical efforts have already been done.[13–16] In the two-orbital systems, Inaba *et al.*[14] and Bünemann *et al.*[16] found that the Mott transition is discontinuous for any finite $J>0$ and continuous only for $J=0$ within a generalized Gutzwiller approximation. However, utilizing the DMFT with the numerical renormalization group, Pruschke and Bulla[15] claimed that the Mott transition is second order for $J>U/4$. They found that the variation of the local squared moment of spin near the transition is too small to judge the order of MIT for large J. By making use of the DMFT with the self-energy functional approach, Inaba and Koga[13] believed that the nature of the Mott transition is first order in all the parameter region for finite J, though they found that the jump of quasiparticle weight is too weak to identify the order of the phase transition when J is large enough. The controversy on the order of the MIT suggests that it is urgent to find a more proper quantity to judge the occurrence and the order of the MIT when J is very large.

Up to date, most of the studies have been focused on the Bethe or the hypercubic lattices. It is not known what the essence of the MIT is in the multiorbital Hubbard model on the frustrated lattices. When the strong electron-electron interactions compete with the geometrical frustration effects, a number of unconventional phases and exotic properties

emerge as the result of the competition, such as the MIT and the antiferromagnetism in the organic compounds κ-(BEDT-TTF)$_2X$ with X as an anion,[17,18] etc. Recent development in material fabrication shows that more and more transition-metal oxides exhibit strong electronic correlation on two-dimensional triangular lattices and the multiple orbital character, such as $NaNiO_2$,[19] and $AgNiO_2$,[20] etc. These appeal for the study on the multiorbital Hubbard model on the triangular lattice.

In this paper, we focus on the MIT physics of the two-orbital Hubbard model on a triangular lattice by means of the exact-diagonalization DMFT. We adopt the local squared moment of charge, together with the local squared moments of spin and orbital, to measure the occurrence of MIT in the two-orbital Hubbard model, and find that we can well judge the occurrence of the MIT when Hund's coupling J is very large. We definitely show that the MIT at large J is first order. The variation of the optical conductivity of the two-orbital Hubbard model is also consistent with the MIT with the increase of U. The rest of this paper is organized as follows: In Sec. II, we describe the model Hamiltonian of the two-orbital system and briefly explain the framework of the exact-diagonalization DMFT approach. In Sec. III, we present the evolutions of the densities of states (DOSs), the local squared moments of charge, spin and orbital, and the optical conductivity with the on-site Coulomb interaction. The order of the MIT in the two-orbital system is also discussed in Sec. III. The last part is devoted to the summary.

II. HAMILTONIAN AND METHOD

We start from a half-filled two-orbital Hubbard model,

$$H = \sum_{\langle i,j\rangle,\alpha,\beta\sigma} t_{\alpha\beta} c^{\dagger}_{i\alpha\sigma} c_{j\beta\sigma} + \sum_i H'_i, \tag{1}$$

$$H'_i = U\sum_{\alpha} n_{i\alpha\uparrow} n_{i\alpha\downarrow} + U'\sum_{\sigma\sigma'} n_{i1\sigma} n_{i2\sigma'} + J\sum_{\sigma\sigma'} c^{\dagger}_{1\sigma} c^{\dagger}_{2\sigma'} c_{1\sigma'} c_{2\sigma} + J'\sum_{\alpha\neq\beta} c^{\dagger}_{\alpha\uparrow} c^{\dagger}_{\alpha\downarrow} c_{\beta\downarrow} c_{\beta\uparrow}, \tag{2}$$

in a triangular lattice, where $c^{\dagger}_{i\alpha\sigma}$ ($c_{i\alpha\sigma}$) is the creation (annihilation) operator of the electron at site i with orbital $\alpha(=1,2)$ and spin $\sigma(=\uparrow,\downarrow)$, and $n_{i\alpha\sigma}$ is the electron number operator. $t_{\alpha\beta}$ denotes the hopping integral from the β orbital to the α orbital, and only the nearest-neighbor hopping is taken into account. For clarity and to compare our results with the present literature, we assume that the intraorbital hopping integrals are the same, i.e., $t_{\alpha\alpha}=t_{\beta\beta}=t=1$ (the energy unit), and we neglect the interorbital hopping, though sometimes the interorbital components may play an important role.[22]

The parameters U, U', J, and J' denote the intraorbital Coulomb, interorbital Coulomb, Hund's, and the pair-hopping couplings. In what follows, considering the realistic wave functions of $3d$ orbitals[23] and the spin rotational symmetry, we adopt the relationships $J=J'$ and $U=U'+2J$. Unlike the Bethe or hypercubic lattice, the particle-hole symmetry is broken at half-filling on the triangular lattice. At $U=0$, the tight-binding dispersion of each orbital channel is

$$\epsilon_{\mathbf{k}\alpha\alpha} = -2t_{\alpha\alpha}\left[\cos(k_x) + 2\cos\left(\frac{\sqrt{3}}{2}k_y\right)\cos\left(\frac{k_x}{2}\right)\right], \tag{3}$$

with the bandwidth $W=9|t|$.

Within the framework of the DMFT, Hamiltonians (1) and (2) are mapped onto an effective Anderson impurity model by integrating over all the spatial degrees of freedom, except for the central site o. The corresponding Hamiltonian H_{eff} contains a central "atomic" or "impurity" part H_{atom} and an effective medium part H_{med}, which has to be determined self-consistently. The two-orbital Anderson impurity Hamiltonian reads

$$H_{\mathrm{eff}} = H_{\mathrm{atom}} + H_{\mathrm{med}}, \tag{4}$$

and

$$H_{\mathrm{med}} = \sum_{\alpha\sigma} \epsilon_{d\alpha} d^{\dagger}_{\alpha\sigma} d_{\alpha\sigma} + \sum_{\alpha\sigma,k=2}^{n_s} \epsilon_{k\alpha\sigma} a^{\dagger}_{k\alpha\sigma} a_{k\alpha\sigma} + \sum_{\alpha\sigma,k=2}^{n_s} V_{k\alpha\sigma}(d^{\dagger}_{\alpha\sigma} a_{k\alpha\sigma} + \mathrm{H.c.}), \tag{5}$$

where $d^{\dagger}_{\alpha\sigma}$ and $a^{\dagger}_{\alpha\sigma}$ create the impurity electron and a bath electron, respectively; the impurity level $\epsilon_{d\alpha}$ is usually chosen as the zero point of energy, and the hybridization parameter $V_{k\alpha\sigma}$ of the impurity model is calculated self-consistently in DMFT. The atomic Hamiltonian H_{atom} of the central site is the same as H' in Eq. (2), and n_s represents the number of the conduction band of the Anderson impurity model. For a set of parameters (U and J), we can obtain the interacting Green's function $G_{\alpha\sigma}(i\omega_n)$, the free Green's function $G_{0\alpha\sigma}(i\omega_n)$, and the self-energy of the Anderson model as follows:

$$\Sigma^{\alpha\beta}_{\sigma}(i\omega_n) = [G^{-1}_{0\sigma}(i\omega_n) - G^{-1}_{\sigma}(i\omega_n)]_{\alpha\beta}, \tag{6}$$

and the lattice Green's function is

$$G^{\alpha\beta}_{\sigma}(i\omega_n) = \sum_{\mathbf{k}} G^{\alpha\beta}_{\sigma}(\mathbf{k}, i\omega_n) \tag{7}$$

$$= \sum_{\mathbf{k}} \left[\frac{1}{i\omega_n + \mu - \epsilon_{\mathbf{k}} - \Sigma_{\sigma}(i\omega_n)}\right]_{\alpha\beta}, \tag{8}$$

and the impurity Green's function $G^{\alpha\beta}_{\mathrm{imp},\sigma}(i\omega) = \langle\langle d_{\alpha\sigma}; d^{\dagger}_{\alpha\sigma}\rangle\rangle_{i\omega}$ is given by

$$G^{\alpha\beta}_{\mathrm{imp},\sigma}(i\omega) = \left[\frac{1}{i\omega + \mu - \epsilon_{d\alpha} - \Delta_{\sigma}(i\omega) - \Sigma_{\mathrm{imp},\sigma}(i\omega)}\right]_{\alpha\beta}. \tag{9}$$

In Eq. (9), the spectral width function $\Delta_{\alpha\sigma}(i\omega) = \Sigma_k V^2_{k\alpha\sigma}/(i\omega+\mu-\epsilon_{k\alpha\sigma})$, μ is the chemical potential, and $\omega_n=(2n+1)\pi/\beta$ is the fermionic Matsubara frequency. Throughout this paper, we fix the temperature $\beta=1/k_BT=16$. We perform the iterative procedure repeatedly until a self-consistent solution of the lattice Green's function and the self-energy is found.

Various analytical and numerical methods can be employed to solve the effective impurity problem. In the following, we first make use of the exact-diagonalization (ED) method to treat the impurity model [Eqs. (4) and (5)] at finite temperatures of β.[2] Then, we perform the iteration on Eqs. (6)–(9) repeatedly until a self-consistent solution is found. Some subroutines, such as the minimizing subroutine which searches for the parameters of the Anderson impurity Hamiltonian and the recommended sequence of subroutines (RS) which is used to diagonalize the Anderson impurity Hamiltonian, are from Ref. 2. In this paper, we take $n_s=6$ for each spin channel. Liebsch found that when $n_s>3$, the converged results qualitatively agree with each other,[24] and the accuracy of the ED ansatz in the single-orbital Hubbard model is well controlled. Demchenko *et al.*[25] had shown that in the absence of particle-hole symmetry, the pole formation and the MIT are independent of each other on the Bethe lattice. So, the quasiparticle weight Z is not suitable for characterizing the occurrence of the MIT. In this paper, we utilize the local squared moments of charge, spin, and orbital and the corresponding local susceptibility to characterize the nature of the Mott transition.

Since the MIT is associated with the localization-delocalization transition of the charge degree of freedom, we measure the MIT with the local squared moments of charge $\langle C^2\rangle$,

$$\langle C^2\rangle = \langle (n-2)^2\rangle,$$

together with the local squared moments of spin and orbital,

$$\langle S_z^2\rangle = \langle (n_\uparrow - n_\downarrow)^2\rangle,$$

$$\langle T_z^2\rangle = \langle (n_1 - n_2)^2\rangle. \tag{10}$$

All of these quantities are relevant to the spin-dependent double occupancy $\langle n_\uparrow n_\downarrow\rangle$ and the orbital-dependent double occupancy $\langle n_1 n_2\rangle$,

$$\langle n_\uparrow n_\downarrow\rangle = \frac{\partial F}{\partial U} = \langle n_{1\uparrow} n_{1\downarrow} + n_{2\uparrow} n_{2\downarrow}\rangle,$$

$$\langle n_1 n_2\rangle = \frac{\partial F}{\partial U'} = \langle (n_{1\uparrow} + n_{1\downarrow})(n_{2\uparrow} + n_{2\downarrow})\rangle, \tag{11}$$

through a few identities, such as

$$\langle C^2\rangle = \frac{\partial F}{\partial \mu} + 2\left(\frac{\partial F}{\partial U} + \frac{\partial F}{\partial U'}\right). \tag{12}$$

Here, F is the free energy and μ the chemical potential. The local susceptibilities of the charge, spin, and orbital are defined by

$$\chi_c = \int_0^\beta \langle \mathcal{T}[n(\tau) - 2][n(0) - 2]\rangle d\tau,$$

$$\chi_s = \int_0^\beta \langle \mathcal{T}[n_\uparrow(\tau) - n_\downarrow(\tau)][n_\uparrow(0) - n_\downarrow(0)]\rangle d\tau,$$

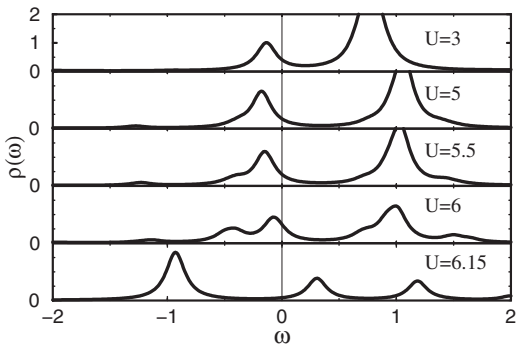

FIG. 1. Evolution of density of states (DOS) $\varrho(\omega)$ with intraorbital Coulomb interaction U in two-orbital Hubbard model on triangular lattice. From top to bottom, $U=3$, 5, 5.5, 6, and 6.15, $J=U/4$, and $\beta=16.0$.

$$\chi_o = \int_0^\beta \langle \mathcal{T}[n_1(\tau) - n_2(\tau)][n_1(0) - n_2(0)]\rangle d\tau, \tag{13}$$

where $\mathcal{T}$ is the time ordered operator, $n(\tau)=\Sigma_{\alpha\sigma} n_{\alpha\sigma}(\tau)$, $n_{\sigma(\alpha)}(\tau)=\Sigma_{\alpha(\sigma)} n_{\alpha\sigma}(\tau)$, and τ is an imaginary time.

With the knowledge of the single-particle energy spectrum, the optical conductivity $\sigma_{xx}(\omega)$ can be calculated in the local approximation.[26–28] In terms of the single-particle spectral weight $A(\mathbf{k},\omega)$, $\sigma_{xx}(\omega)$ is

$$\sigma_{xx}(\omega) = \frac{e^2\pi}{\Omega}\int_{-\infty}^{\infty} d\varepsilon \frac{f(\varepsilon) - f(\varepsilon+\omega)}{\omega} \times \frac{1}{N}\sum_{\mathbf{k}\sigma}\left(\frac{\partial \varepsilon_{\mathbf{k}}}{\partial k_x}\right)^2 A(\mathbf{k},\varepsilon)A(\mathbf{k},\varepsilon+\omega), \tag{14}$$

where e is the electron charge, Ω is the volume of the lattice, and $e^2\pi/\Omega$ is the unit of the conductivity. The disappearance of the Drude peak could indicate the occurrence of MIT, and the optical conductivity peaks provide much information of the charge excitation between subbands of the systems.

III. RESULTS AND DISCUSSION

As reported in the literature, Hund's coupling plays an important role in controlling the Mott transition, and the nature of the Mott transition in the two-orbital system on the E_F symmetric Bethe lattice has been controversial.[13,15] In the present study, we investigate the properties of the Mott transition on the asymmetric triangular lattice so as to resolve the controversial results.

Remarkably different from the Bethe lattice, the DOS of quasiparticles on the triangular lattice is asymmetric, as shown in Fig. 1, where we also present the evolution of the DOS with the increase of the intraorbital Coulomb interaction. For $J=U/4$, it is clearly seen that the Mott transition has already occurred at $U\simeq 6.15$. A detailed numerical calculation shows that the critical value of the MIT is $U_c=6.12$. For other finite J, the dependence of DOS on the Coulomb interaction strength U exhibits a similar tendency. With the increase of Hund's coupling J, the critical points of

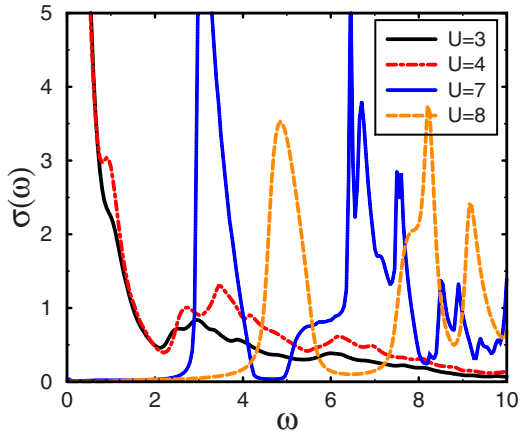

FIG. 2. (Color online) Dependence of optical conductivity on frequency in two-orbital Hubbard model on triangular lattice. The intraorbital interactions $U=3$, 4, 7, and 8 and $J=U/4$; the other parameters are the same as Fig. 1.

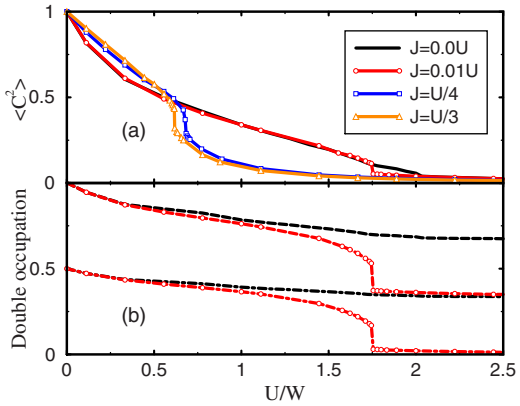

FIG. 3. (Color online) (a) Local squared moment of charge as a function of interaction strength U/W for $J=0.0$, $0.01U$, $U/4$, and $U/3$. (b) Dependence of double occupations $\langle n_\uparrow n_\downarrow \rangle$ (dashed line) and $\langle n_1 n_2 \rangle$ (dot-dashed line) on U for $J=0.0$ and $J=0.01U$ (circle).

the Mott transition occur at 18.2, 16.8, 6.12, and 5.85 for $J=0.0$, $0.01U$, $U/4$, and $U/3$, respectively. The tendency of U_c substantially decreasing with the increase of Hund's coupling on the present two-dimensional triangular lattice is consistent with the previous results on the Bethe lattice. It is very interesting that for various J, the critical value U_c of the MIT on the triangular lattice is about twice larger than that on the Bethe lattice. This may arise from two facts: One is from the spin frustration and fluctuation effect on the triangular lattice and another is from the fact that the orbital fluctuations in the two-orbital system enhance the metallic character, leading to a large critical value U_c.

The optical conductivity also exhibits signatures of the MIT. It is interesting how the optical conductivity evolves with the Coulomb interactions in the two-orbital Hubbard model on the triangular lattice. Compared with that of the single-orbital Hubbard model, the optical conductivity of the two-band Hubbard model is more complicated and exhibits multipeak structure, as seen in Fig. 2. When the Coulomb interaction U is smaller than the critical value U_c, the Drude peak and the charge excitation peaks exist at the same time. The multipeak charge excitation structure in the present system significantly differs from the single-peak structure of the single-orbital Hubbard model.[26] The peaks at $\omega=3.0-3.5$ and $\omega=6.0-6.5$ come from the excitation between different Hubbard subbands below and above the Fermi surface. With the increasing of the Coulomb interaction, the intervals of these Hubbard subbands become larger and larger, and the charge-excitation peaks move to the high frequency, as seen in Fig. 2. Since the bandwidths of the two orbitals are identical, no orbital selective Mott transition is observed. As $U>3$, we observe a small low-energy midpeak at $\omega\sim 1.0$. Such a midpeak may contribute from the quasiparticle peaks near the Fermi level, as seen in the DOS near E_F in Fig. 1. The excitation between the renormalized quasiparticle peaks and the Hubband subbands close to E_F gives rise to this small midpeak. When the Coulomb interaction U is greater than the critical interaction U_c, the Drude peak and the small midpeak disappear. Subsequently, the system enters an insulating phase, as shown in Fig. 2. The insulating gap becomes more and more wide with the increase of the Coulomb interaction. To date, the optical conductivity experiment on the compounds with two orbitals and triangular lattice is not available; we anticipate the corresponding experimental results can be done in the near future.

As known from the earlier literature, Hund's coupling J plays a key role in controlling the nature of the Mott transition in the two-orbital Hubbard model on the Bethe and the hypercubic lattices. On the present triangular lattice, we investigate the local squared moment of charge and the double occupations $\langle n_\uparrow n_\downarrow \rangle$ (the dashed lines) and $\langle n_1 n_2 \rangle$ (the dot-dashed lines) on the intraorbital Coulomb interaction at different Hund's coupling J, as shown in Fig. 3. At $J/U=0$, as seen in Figs. 3(a) and 3(b), there is no singular jump in $\langle C^2 \rangle$, $\langle n_\uparrow n_\downarrow \rangle$, and $\langle n_1 n_2 \rangle$ in this triangular frustrated system, which implies that the Mott transition in the two-orbital system with equal bandwidths is second order. On the other hand, when Hund's coupling J is introduced, there are discontinuous jumps in $\langle C^2 \rangle$ and the double occupancies, as shown in Figs. 3(a) and 3(b), showing that the Mott transition in the two-orbital Hubbard model is first order. This result is consistent with that obtained via the Gutzwiller method[16] on the infinite-dimensional hypercubic lattice. On the Bethe lattice, the jump of $\langle S_z^2 \rangle$ is obscure and it is hard to distinguish whether the MIT is first or second order,[13,15] while on the present triangular lattice, the jumps of the local squared moments of charge $\langle C^2 \rangle$ is very obvious for all $J \neq 0$. Therefore, the MIT in the half-filled two-orbital Hubbard model on the triangular lattice is first order for all finite J situations. These results also agree with those of Inaba and Koga by the DMFT with the self-energy functional approach.[13] However, at $J=U/4$, our result is in contrast to that of Pruschke and Bulla which is obtained by the DMFT with the numerical renormalization group.[15] This shows that $\langle C^2 \rangle$ is a proper measure to the MIT in the large J situation.

To understand the nature of the Mott transition more clearly, we also calculate the local orbital and spin squared moments of $\langle T_z^2 \rangle$ and $\langle S_z^2 \rangle$, as shown in Fig. 4. In the metallic

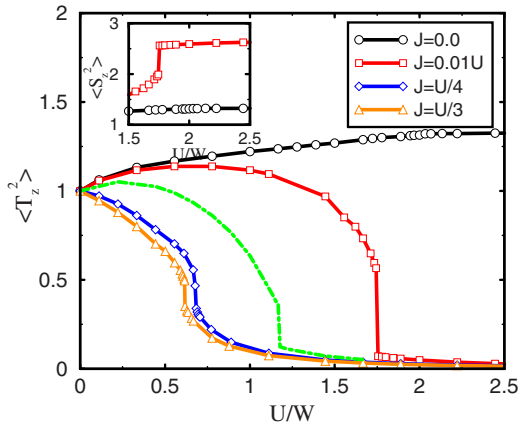

FIG. 4. (Color online) Local orbital squared moment vs ratio of intraorbital Coulomb interaction U over bandwidth W for different J. The green dot-dashed line is for the SU(2) $\otimes$ SU(2) system with $J'=0$, $J=0.1$, and $U=U'+J$. The local spin squared moment vs U/W is shown for $J=0.0$ and $J=0.01U$ in the inset.

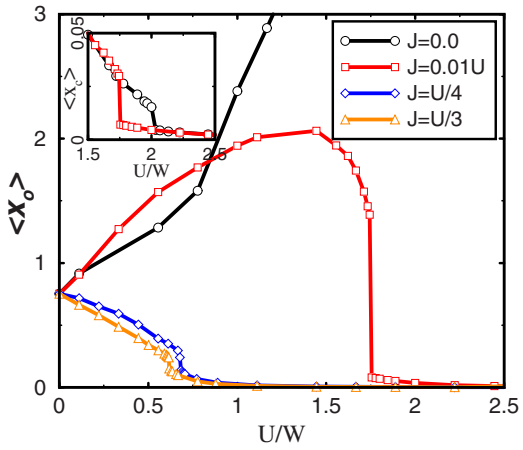

FIG. 5. (Color online) Local orbital susceptibility vs ratio of Coulomb interaction U over bandwidth W for $J=0.0$, $0.01U$, $U/4$, and $U/3$. The inset shows local charge susceptibility in the case of $J=0.0$ and $J=0.01U$, respectively.

limit of $U=0$, the local squared moments $\langle T_z^2\rangle=\langle S_z^2\rangle=1$, and in the insulating and strongly correlated regime, $\langle T_z^2\rangle=\langle S_z^2\rangle=4/3$ for $J=0$, and $\langle T_z^2\rangle=0$ and $\langle S_z^2\rangle=8/3$ for all finite J, which are in agreement with the linearized DMFT results.[29] As seen in Fig. 4, the local squared moments of spin and orbital are continuous at $J=0$, showing that the MIT is second order, in agreement with the result from the local square moment of charge. Further, as seen in Fig. 4, for various finite J with $J=0.01U$, $U/4$, and $U/3$, the discontinuous jumps of the local squared moments of orbital and spin also demonstrate that the MIT is first order, consistent with the preceding results. Therefore, combining the local squared moment of charge $\langle C^2\rangle$ and those of spin and orbital, $\langle S_z^2\rangle$ and $\langle T_z^2\rangle$, one can measure the order of the MIT over all of Hund's coupling J.

Consistent with the behaviors of the local squared moments, the divergence of the local orbital susceptibility near U_c in Fig. 5, together with the discontinuous jump of the local charge susceptibility in the inset in Fig. 5, clearly shows that the MIT on the triangular lattice is second order at $J=0$. Since the MIT in the present system with finite J is first order, the local orbital and charge susceptibilities also exhibit discontinuities. It is worth noticing that due to the frustration effect on the present triangular lattice, the local orbital susceptibility in the system with $J=0.01U$ is suppressed near the MIT critical point; meanwhile, such suppression is observed only for $J=0.03U$ on the Bethe lattice.[13] Similar behavior is also observed in the local squared moment of orbital.

Compared with the single-orbital Hubbard model on the triangular lattice, the critical value U_c of the two orbital model much larger than that in the single-orbital model[21] is mainly due to the orbital fluctuations. The physical origin of the different order in the MIT systems with finite J and $J=0$ is still a puzzle. Bünemann *et al.* attributed it to the presence of multiple atomic energy scales in the two-orbital Hubbard model. This argument may be not true since there does exist more than one atomic energy scale except U in the single-orbital Hubbard model. To resolve this puzzle, we suggest that the order of MIT in the strongly correlated Hubbard model may depend on the symmetry of the systems. At $J=0$, the spin-orbital coupling system is SU(4) symmetric; on the other hand, the rotational symmetry of the orbital space is usually broken for finite J. Even if the rotational symmetry of the orbitals exists, i.e., $U=U'+J$ and the interorbital Hund's coupling $J'=0$, the symmetry of the system is SU(2) $\otimes$ SU(2). However, we find that the phase transition in such a system is still first order, as seen in the green curve (dot-dashed line) in Fig. 4. We also notice that in the two-orbital Hubbard model with the same bandwidths, the OSMT is excluded. It is interesting to ask what the order of the OSMT is in the two-orbital triangular Hubbard models with different bandwidths, which deserves further study.

One notes that in the two-dimensional triangular spin systems, the geometric frustration is considerable in the strong correlation regime, so the spatial correlations and fluctuations of spins may be important. In this situation, the approximation and precision of the present single-site DMFT approach should be carefully justified. Fortunately, when we constrain the discussion in the paramagnetic phases, the precision of such an approximation is well controlled. This has been demonstrated for the single-orbital Hubbard model in the triangular lattice by several authors.[21,30] Aryanpour *et al.*[21] and Merino *et al.*[30] have shown that the results of the single-orbital Hubbard model obtained by the single-site DMFT approach are consistent with those by other methods. The transport properties of the two-dimensional triangular Hubbard model within the single-site DMFT agrees with the experimental results of the organic compound.[31] On the contrary, such a method fails when it is applied for the two-dimensional square lattice. This arises from the fact that in the two-dimensional triangular lattice, the spatial antiferromagnetic correlation is greatly suppressed by the geometric frustration, as pointed out by Aryanpour *et al.*[21] and Merino *et al.*[30] Another reason is that the coordination number of the triangular lattice is considerably larger than that of the square lattice.

On the other hand, it is highly desirable to extend the present single-site DMFT approach to the cluster or cellular DMFT approach so as to well incorporate the spatial fluctuation and the intersite correlation, as developed by many authors for the single-orbital models in recent years.[32–36] However, such an extension to the multiorbital model meets difficulty since it goes beyond the ability of the high-performance computing resources available. We anticipate that the cluster extension will not qualitatively affect our conclusions.

IV. CONCLUSIONS

By using the exact-diagonalization DMFT approach, we have demonstrated that Hund's coupling J leads to a first-order metal-insulator transition in the two-orbital Hubbard model with the degenerate bandwidths in the triangular lattice. The discontinuities of the local squared moments of the charge, spin, and orbital show that the first-order metal-insulator transition occurs not only in the small J region but also in the large J region. Such distinct behaviors of the systems with finite J and $J=0$ are attributed to the lowering of the symmetry of the systems. The multipeak structure in the optical conductivity of the two-orbital Hubbard model arises from the charge excitation among more than two Hubbard subbands.

ACKNOWLEDGMENTS

This work was supported by the NSFC of China No. 90303013, by the BaiRen Project, and by the Knowledge Innovation Program of the Chinese Academy of Sciences. Part of the calculations were performed at the Center for Computational Science of CASHIPS and the Shanghai Supercomputer Center.

[1] M. Imada, A. Fujimori, and Y. Tokura, Rev. Mod. Phys. **70**, 1039 (1998).
[2] For a review, see A. Georges, G. Kotliar, W. Krauth, and M. J. Rozenberg, Rev. Mod. Phys. **68**, 13 (1996), and some references thereafter.
[3] G. Kotliar and D. Vollhardt, Phys. Today **57** (3), 53 (2004).
[4] R. Bulla, T. A. Costi, and D. Vollhardt, Phys. Rev. B **64**, 045103 (2001).
[5] R. Bulla, Phys. Rev. Lett. **83**, 136 (1999).
[6] S. Onoda and M. Imada, J. Magn. Magn. Mater. **272-276**, E275 (2004).
[7] K. I. Kugel and D. I. Khomskii, Sov. Phys. JETP **37**, 725 (1973); Y. Tokura and N. Nagaosa, Science **288**, 462 (2000).
[8] V. I. Anisimov, I. A. Nekrasov, D. E. Kondakov, T. M. Rice, and M. Sigrist, Eur. Phys. J. B **25**, 191 (2002).
[9] A. Koga, N. Kawakami, T. M. Rice, and M. Sigrist, Phys. Rev. Lett. **92**, 216402 (2004).
[10] A. Liebsch, Europhys. Lett. **63**, 97 (2003).
[11] A. Liebsch, Phys. Rev. Lett. **91**, 226401 (2003).
[12] A. Liebsch, Phys. Rev. B **70**, 165103 (2004).
[13] K. Inaba and A. Koga, Phys. Rev. B **73**, 155106 (2006); J. Phys. Soc. Jpn. **76**, 094712 (2007).
[14] K. Inaba, A. Koga, S.-I. Suga, and N. Kawakami, Phys. Rev. B **72**, 085112 (2005).
[15] Th. Pruschke and R. Bulla, Eur. Phys. J. B **44**, 217 (2005).
[16] J. Bünemann and W. Weber, Phys. Rev. B **55**, 4011 (1997); J. Bünemann, W. Weber, and F. Gebhard, *ibid.* **57**, 6896 (1998).
[17] K. Kanoda, Physica C **282-287**, 299 (1997); Hyperfine Interact. **104**, 235 (1997).
[18] R. H. McKenzie, Science **278**, 820 (1997).
[19] L. Petit, G. M. Stocks, T. Egami, Z. Szotek, and W. M. Temmerman, Phys. Rev. Lett. **97**, 146405 (2006).
[20] E. Wawrzynska, R. Coldea, E. M. Wheeler, I. I. Mazin, M. D. Johannes, T. Sörgel, M. Jansen, R. M. Ibberson, and P. G. Radaelli, Phys. Rev. Lett. **99**, 157204 (2007).
[21] K. Aryanpour, W. E. Pickett, and R. T. Scalettar, Phys. Rev. B **74**, 085117 (2006).
[22] Y. Song and L.-J. Zou, Phys. Rev. B **72**, 085114 (2005).
[23] C. Castellani, C. R. Natoli, and J. Ranninger, Phys. Rev. B **18**, 4945 (1978).
[24] A. Liebsch, Phys. Rev. Lett. **95**, 116402 (2005).
[25] D. O. Demchenko, A. V. Joura, and J. K. Freericks, Phys. Rev. Lett. **92**, 216401 (2004).
[26] M. J. Rozenberg, G. Kotliar, H. Kajueter, G. A. Thomas, D. H. Rapkine, J. M. Honig, and P. Metcalf, Phys. Rev. Lett. **75**, 105 (1995).
[27] A. Khurana, Phys. Rev. Lett. **64**, 1990 (1990).
[28] M. Jarrell, J. K. Freericks, and Th. Pruschke, Phys. Rev. B **51**, 11704 (1995).
[29] Y. Ono, M. Potthoff, and R. Bulla, Phys. Rev. B **67**, 035119 (2003).
[30] J. Merino, B. J. Powell, and R. H. McKenzie, Phys. Rev. B **73**, 235107 (2006).
[31] P. Limelette, P. Wzietek, S. Florens, A. Georges, T. A. Costi, C. Pasquier, D. Jerome, C. Meziere, and P. Batail, Phys. Rev. Lett. **91**, 016401 (2003).
[32] E. C. Carter and A. J. Schofield, Phys. Rev. B **70**, 045107 (2004).
[33] K. Haule and G. Kotliar, Phys. Rev. B **76**, 104509 (2007).
[34] M. S. Laad and L. Craco, arXiv:cond-mat/0701585 (unpublished).
[35] B. Kyung, G. Kotliar, and A.-M. S. Tremblay, Phys. Rev. B **73**, 205106 (2006).
[36] Y. Z. Zhang and Masatoshi Imada, Phys. Rev. B **76**, 045108 (2007).